Robust Optimization Framework for Economic Dispatch of DER and BES Based Micro Grid Considering a Voltage Dependent Load

Kumar, Ramesh
School of Renewable Energy and Efficiency, National Institute of Technology

Sharma, Rahul
Electrical Engineering, National Institute of Technology

Kumar , Ashwani
Electrical Engineering, National Institute of Technology

https://doi.org/10.5109/7160911

出版情報：Evergreen. 10 (4), pp.2325-2338, 2023-12. 九州大学グリーンテクノロジー研究教育センター
バージョン：

Robust Optimization Framework for Economic Dispatch of DER and BES Based Micro Grid Considering a Voltage Dependent Load

Ramesh Kumar[1], Rahul Sharma[2], Ashwani Kumar[2]

[1]School of Renewable Energy and Efficiency, National Institute of Technology, Kurukshetra, India

[2]Electrical Engineering, National Institute of Technology, Kurukshetra, India

*Author to whom correspondence should be addressed:

E-mail: redhuramesh98@gmail.com

(Received July 29, 2023; Revised September 29, 2023; accepted October 6, 2023).

Abstract: Energy storage devices (ESS) and distributed generations are integrated or characterized with the help of distribution networks (ADNs). Micro grids (MGs) are ADNs but they can also operate in stand-alone mode. Micro grid provides redress to several factors in the power quality systems by integrating renewable and non-renewable Distributed Energy Resources along with Energy Storage Systems. A robust optimization framework for economic dispatch (ED) for such a micro grid is proposed in this paper. In this paper, modified IEEE 24 bus model of mess distribution including energy resources that are intermittent such as photovoltaic (PV) energy source, wind turbines, include conventional diesel generators, battery energy storage (BES) systems are essential components of hybrid energy systems. PV units convert sunlight into electricity while wind turbines harness power from the wind systems store excess energy generated has been considered to implement the proposed optimized algorithm. In this technique, micro grid is heavily loaded or operated in islanded mode to realize that the local generation and Because of the penetration of distributed energy resources, system operators can meet this high demand for heavy loads with no need to purchase additional power from the grid. A time varying voltage dependent load model has been considered for obtaining the optimal economic dispatch for an IEEE test system. The impacts of Battery energy and distributed energy system penetration has also been considered. The voltage deviation is minimized while taking the technical constraints of alternate current optimal power flow (OPF) into account. In addition, the paper also considers conservation voltage reduction (CVR) with the aim to optimally schedule reactive power from inverters for voltage regulation support and BES's charging/discharging. The problem is solved under different scenarios and examined within a 24 hour (h) time horizon. The results are obtained for different scenarios and discussed to reflect the effectiveness and efficiency of the proposed optimization technique.

Keywords: Micro grid, Distributed Energy Resources,(DER), Diesel generator, Solar, Photo Voltaic, Wind, Battery Energy Storage, Time Varying Voltage Dependent Load, Economic Dispatch, Optimal Power Flow, Robust Optimization, Active Distribution Network(ADN).

1. Introduction

1.1 Background and motivation

At present, the development in the power sector is basic need of life as for the survival in human being. For development in the power sector, different methods are being utilized such as electric utility with proper channel, rule regulation decentralization and proper distribution of the power with dynamically changing control system in the electricity market. Distributed energy resources are used for power generation using the different techniques like as micro-turbine, fuel cell, photo voltaic units, wind turbine[1)] , diesel engines gas turbines[2)] and storage technologies like flywheel, compressed air energy storage (CAES),Super conducting magnet energy (SMES), super capacitors and batteries. At present, the renewable energy-based DG is rapidly integrated into AND hence DERs have become an integral component of the system. Such growing penetration of RES also comes with new technical challenges such as voltage fluctuation and frequency and imbalance power flow violation problems to the power grid[3)]. Power system blackout during the demand of the electricity is also one of the major issues to look for the alternatives[4)]. It is quite challenging to incorporate the intermittent energy sources scheduling with the already installed thermal plants or solar system.

Using of the thermal efficiency parabolic dish concentrator for cooking is part of renewable energy [5]Two of the widely used and exploited renewable energy technologies are wind and solar have been taken into consideration in this study[6] for improvement in the power system by integrating the power flow unified controller in the power network[3]. Dispatching renewable power in network is a challenge due to the irregular behaviour of the Renewable energy sources (RES). RES are affected by temp., weather condition, air flow & humidity. Imbalance of the power frequency[7] and fluctuations in the voltage and line losses are the main factors to control during generation and load dispatch[8]. This is one of the major issues while interfacing them with MG and involves compromising with the economic dispatch model in proper structuring[9]. The maintaining load balance becomes problematic with the increase of RES penetration in power network. The percentage of penetration of RES would directly reflect the affected scenario of the load balancing. Energy storage systems (ESS) are incorporated to mitigate the uncertainty caused by RES and provide voltage regulation support[10]. Different inverter used for the high quality power supply in the ac and dc micro grid. Then using the several method used in the balance voltage stability and frequency stability for the hybrid micro grid[11] .The inverters for DGs are designed to provide DC output suitability for storage, real-time reactive power control and voltage regulation services by active power curtailment[12]. Since operation and efficiency of the ADN is significantly affected by location and capacity of DG and BES; optimal planning of DG and BES is required to fully harvest their potential in the MG. Several advantages of the integration of the DER with grid have presented in literature of this field[13]. The policy drivers also giving significant boost to MGs because of stringent rules regarding environmental concerns, pollution in the developed and developing countries where governments are revising their policies. Therefore, resolving the power dispatch challenge with RES and energy storage technologies has thus become necessary. Information on the optimum economic output of the sources is must in a network that can support the load and provide the solution to the economic dispatch issue. Integration of electrical vehicle[14] . Also studied about the wind energy potential about the site their cost, size and technical analysis[15].

1.2 Related Work

Economic dispatch issues with PV and wind power instability has been discussed[16]. The variability of wind power output is explained using a stochastic method based on possibilities, and programming solutions founded for each situation[17]. Nevertheless, the issue of wind thermal-dynamic ED and the amount of accessible wind energy calculated[18] is solved taking into consideration probability distribution function as Weibull probability distribution function (PDF). In this analysis, a Weibull PDF distribution function of the wind speed and daily normal irradiance (DNI) of solar PV system[7] for solving an economic dispatch model is considered and utilizes the both wind and solar systems output by considering their stochastic nature.Literature on BES and DG expansion planning in ADN is discussed in this section. Aforementioned works are focused on either BES or DG allocation optimization problems[19], else the problem is solved BES's allocation problem under existing DG resources. Design of the problem of DG and BES are considered. Distributed generation and the uncertainty model of renewable enbergy sources is divided into three types[20] as stochastic scenarios, uncertainty set, and probabilistic model. Sensitivity analysis, dynamic programming and meta-heuristic algorithms have been utilized in order to solve the planning and operation problem. In the aforementioned work, voltage regulation capability and reactive power utilization from Distributed Generation inverters are rarely considered.Additionally, a Micro grid is inherently a distribution network. Transmission systems have large number of generators connections, long length of balanced and transposed cables covering a wide area. In contrast, distribution systems are relatively localized. In technical terms, distribution networks have radial topology, high R/X ratio of the lines which are not transposed and unbalanced loading at different phases. Considering these factors, the Distribution generation power fluctuation or disturbance may be strongly affect the voltage stability in Micro Grid. Owning to these reasons, load flow methods are used for analyzing transmission network may not converge or may give false results in case of a distribution network. The distribution system power flow utilizes unified flow methods that are highly depending upon the characteristics and the topology of the network[21]. In,[22] complete evaluations of several processes are utilized to share of loss in a distribution system under the market environment.Nowadays, the inverter interfaced DGs can provide reactive power compensation due to the improvement of power electronics inverter technology and their control systems. Such inverters provide voltage support and regulation depend on its fast reactive power injection/consumption capability. DG inverter rating and type determines it's active and reactive power output. To further utilize inverter's reactive power capacity the concept of DG "inverter over-sizing" has introduced[23][24] A voltage dependent load decreases with a drop in the voltage supply across it. Hence, it is recommended to maintain the voltage magnitude to the minimum limit to maintain or reduce the load demand. Such energy saving scheme is called conservation voltage reduction (CVR). Utilities can get benefited not only by loss reduction and peak load shaving but also by government incentives for increased social welfare from environment conservation when CVR is implemented[25]. On implementing CVR and Distribution generation, simultaneously new energy savings is achieved[26]. Effects of CVR operation are

discussed in[27]. DG location and CVR operation is solved concurrently in[26] using a two-stage stochastic optimization framework. In, the impact of CVR with DG active/reactive power control was investigated under various saturation points of RES. By monitoring the on-load-tap changer (OLTC), voltage controllers, Photovoltaic inverters and capacitor energy banks, and a closed loop control scheme for CVR is implemented[28] . A stochastic optimal Battery Energy System are planning framework considered CVR is proposed for ADN having abundant RES. Hence, for the planning aspects, coordinated voltage control support from Distribution generation or Battery Energy System for CVR must be studied. In addition, inverter over-sizing should be implemented to improve voltage regulation.elctrical vechicle managment sytem and improvemnt[14]

1.3 Contribution of this paper

This paper represent an efficacious robust optimization technique to optimally panel the diesel generators and other load dispatch centers for economic integration of renewable energy sources adhering reactive power constraints of the network. The main contributions of this work are as follows:

The technique recommends optimal operation of all the RER accessible in the MG and meticulously studies characteristics like voltage enhancement and power loss reduction. AC optimal power flow (OPF) has been utilized to obtain Micro grid's state variables.

A novel cost function for minimizing voltage deviation has been included in the expanse function.

For proper management of voltage in micro grid, the methodology identifies the weak generators to provide them the sufficient support required. If problems arise due to weak generation, load shedding is opted to achieve desired operating conditions whenever it is feasible and economical.

Proposing an economic dispatch model (EDM) to integrate renewable energy resources in the Micro-grid, the uncertainty of wind and solar energy resources are taken into consideration. The advanced methodology maximizes the conversion of renewable power into active power so that maximum savings can be achieved in the fuel cost.

Parameters like LMP and congestion cost which are helpful in monitoring and maintaining the system performance even in the worst possible contingency, are defined and analyzed.

Instead of a static load, a time varying voltage dependent load has been simulated and hence CVR is achieved.

There will be finally incorporation of the different cases with purposed model for emphasizing the correctness, effectiveness and robustness in the ac optimal power supply.[29]However, regarding the constraints to be considered for optimal operation, this technique has not considered the limits at all ends such as the active power of a distribution transformer, the active power at home level and the main circuit breaker at home. Exceeding total power may result in an overload on the distribution transformer (DT) and may reduce overall life of the equipment's and increase the economical losses.

1.4 Outline of this paper

This paper is categorized as five sections: ED problem statement is formulated taking into account the model of integrated renewable energy sources based systems in Section 2. Section 3, has provided the dataset and the particular information of each case study that are analyzed. The results are obtained using Mat lab simulation platform and the results are explained in Section 4. Section 5, finally, presented the summary of the paper.

2. Problem Formulation

The formulation of economic dispatch problem with the distributed renewable energy resource taking cost minimization function is designed by considering three key costing components into account. The objective function is written as equation (1) consists of operating and installation expenses of diesel generator units (DGU), load shedding prices, renewable energy deduction expanses and expanses of voltage deviation. In this part, an optimal model while considering all the constraints is described below.

Expanse Function

$$\min_{P_i^{th},P_{i,t}^{wc},Lsh_{i,t}} \quad OF = F^{th} + F^{wc} + F^{Lsh} + F^{Vdev} \tag{1}$$

Where F^{th} is the expanse of producing units, F_{wc} is the wind restriction price, F_{Lsh} is the price of load shedding and F_{Vdev} is the expanse of voltage deviation.

$$F^{th} = \sum_{g,t} a_g . P_{g,t}^2 + b_g . P_{g,t} + c_g \tag{2}$$

F^{th} is a quadratic function which represents the active power output of the diesel generator $P_{g,t}$ (kW) for the purpose of good fuel price curve estimation [39]. The parameters of the diesel generator considred are, a [R_s/(kW2h)], b [R_s/(kWh)] and c [R_s/h], and these parameters are obtained from the heat run test during the analysis of the results from the input and output measurements data.

$$F^{wc} = VWC \times \sum_{i,t} (P_{i,t}^{wc} + P_{i,t}^{sc}) \tag{3}$$

F_{wc} represent the linear function of deducted renewable power $P_{i,t}^{wc}$ and $P_{i,t}^{sc}$ at i^{th} bus during t^{th} hour [30]. However, renewable power deduction comes into effect when either the network is lightly loaded up to the limit at which all the generators are running at their minimum generation and excess renewable power is available or if the generators are unable to ramp down when there is sudden drop in load. There are two alternatives to mitigate the wind reduce cost (i) load-shifting technique (ii) Optimal battery sizing along with the wind farm.

$$F^{Lsh} = VOLL \times \sum_{i,t} Lsh_{i,t} \tag{4}$$

The equation F^{Lsh} is linear function of load shed ($L^{shi,t}$)

at i^{th} bus and t^{th} time interval as in [40]. Inconvenience brought on by some customers' inability to access power must be assessed against the operating agent. To supply emergency loads (such as hospitals) and priority loads (such as research labs), however, a sufficient power reserve should be maintained

$$.F^{Vdev} = VDV \times \sum_{i,t}\left(1 - v_{i,t}\right)^2 \quad (5)$$

F^{Vdev} is the quadratic function of voltage deviation. 1 p.u. is the nominal value of voltage, hence (1-$v_{i,t}$) is the abnormality from the nominal value. The above cost function provides a simple mathematical equation to consider the penalty to be imposed on network operator for deviation in voltage.

2.1 Diesel Generators

The thermal power plant constrains with the plant capacity is represented by

$$P_g^{min} \le P_{g,t} \le P_g^{max} \quad (6)$$

In addition, the power flow for alternate current (AC) lines, limits for generator reactive power are also to be considered as:

$$Q_g^{min} \le Q_{g,t} \le Q_g^{max} \quad (7)$$

The constraints of tghe ramp-up and ramp-down equations for the generator active power output is represented by

$$P_{g,t-1} - P_{g,t} \le RD_g \quad (8)$$

$$P_{g,t} - P_{g,t-1} \le RU_g \quad (9)$$

.

2.2 Wind Turbines

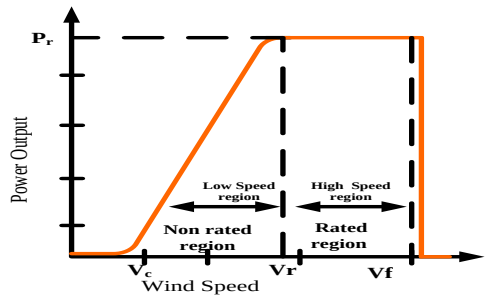

Fig. 1: Power output curve of Wind system

The Fig 1. is show the cubic model of wind power curve & equations below[31].

$$\begin{cases} P^r \times \left(\frac{v - v_{in}}{v_r - v_{in}}\right)^3; & v_c \le v \le v_r \\ P^r; & v_{r \le} v \le v_f \\ 0; & v < v_c \; or \; v > v_f \end{cases} \quad (10)$$

where, $P^r$and P^w is rated & actual wind power output at wind speed v. Cut in and cut out limits of the wind are v_c and v_f and the minimum wind velocity is v_r at which rated power is generated. The defined fractional availability of wind $w_{i,t}$ which is calculated by using wind speed data for 24 hours.

$$w_{i,t} = P_{i,t}^{w,avl} / W_i^{cap} \quad (11)$$

Where W_i^{cap} is analogous to P_i^r and is connected at i^{th} bus. The calculated power of the wind system is given by

$$P_{i,t}^{wc} = w_{i,t} \times W_i^{cap} - P_{i,t}^w \quad (12)$$

The capacity constrain of wind turbine is given by

$$0 \le P_{i,t}^w \le w_{i,t} \times W_i^{cap} \quad (13)$$

The maximum wind power output is different at each bus, which is givenW_i^{cap}. Hence, inequality (13) follows for the actual power output of wind farm. Because the wind curve of the farm, have the same shape or cut in cut out of the velocity in the wind turbine.

Photo- voltaic (PV) based unit

The solar power is calculated by the solar irradiance which is obtained from the PV (I_t),

$$I_t = I_d \times \cos\theta_\beta + I_{dif} \times \frac{(1+\cos\beta)}{2} + \rho \times I_g \times \frac{(1-\cos\beta)}{2} \quad (14)$$

Where, I_d & I_{dif} is used for direct normal irradiance (DNI), diffuse horizontal irradiance (DHI), I_g, β , ρ & θ_β is used to represent the global horizontal irradiance (GHI), the tilted angle, surrounding reflection, and incidence angle of solar radiation on the tilted surface. Photovoltaic power generated in the power the system at i^{th} bus during t^{th} hour $P_{i,t}^{PV}$ can be calculated as.

$$P_{i,t}^{PV} = P_{stc}^{PV} \times n_s^{PV} \times n_p^{PV} \times (I_t/1000) \times [1 - \in (T_t^c - 25)] \quad (15)$$

Here P_{stc}^{PV} the highest power point of a photovoltaic unit's output under established test conditions, n_s^{PV} and n_p^{PV} are solar PV panels installed in combination of series and parallel respectively, $\in$, T_t^c is the temperature coefficient and 25℃ is taken as the standard temperature.

Solar PV Cell temperature is proportional with respect to the ambient temperature which is expressed in the equation below [43]

$$T_t^c = T_t^a + (I_t/800) \times (NOTC - 20) \quad (16)$$

In the equation, T_t^a is the ambient temperature and NOTC is the nominal temperature of the solar PV cell. The fractional availabilioty of the solar powet is dened n i (17) as $s_{i,t}$ and is expressed as

$$s_{i,t} = P_{i,t}^s / S_i^{cap} \quad (17)$$

Where S_i^{cap} is simi;lar to maximum power output of the PV unit connected at ith bus. The values of $s_{i,t}$ is determined for each hour using above model and the irradiance data (Fig. 2).

($P_{i,t}^s \approx P_{i,t}^{PV}$) Power output of the converter ($P_{i,t}^s$) should be within the rated capacities as follows:

$$0 \le P_{i,t}^s \le s_{i,t} \times S_i^{cap} \quad (18)$$

The V-I characteristics of all the solar panels have same shape and same parameter, but the maximum power of the converter is different in he every bus because it depended on the solar farm size and hence the maximum power output of the converter is different at each bus. Which is represented S_i^{cap}. Hence inequality (18) follows for the actual power output of solar farm follows

2.3 Battery model

The battery storage systems are used as a backup to Renewable energy resources as these storage devices can supply power when the availability from the RES is not adequate. In this model, the state of charge has calculated for each battery[32]. The study utilized a well-established optimization technique to determine the optimal Depth of Discharge and nominal capacity for a battery. The technique considers various factors such as battery life, efficiency, cost and Depth of Discharge (DOD)

$$SOC_i^{min} = C_i^{nb}(1 - DOD_i^{max}) \quad (19)$$

$$SOC_i^{max} = C_i^{nb} \quad (20)$$

$$SOC_{i,t} = SOC_{i,t-\Delta t}.\left(1 - DOD_{i,t}\right) + \left(P_{i,t}^{ch}.\eta_{ch} - P_{i,t}^{dis}.\frac{1}{\eta_{dis}}\right).\Delta t \quad (21)$$

Constraints for S_{OC}, charging and discharging limits for battery are given by

$$SOC_i^{min} \le SOC_{i,t} \le SOC_i^{max} \quad (22)$$

$$P_{i,t}^{ch,min} \le P_{i,t}^{ch} \le P_{i,t}^{ch,max} \quad (23)$$

$$P_{i,t}^{dis,min} \le P_{i,t}^{dis} \le P_{i,t}^{dis,max} \quad (24)$$

2.4 Load model

Shedding of non-critical load becomes necessary in these situations because there will be times when generated power is not enough to meet the load..The i, t is the value of load shedding at bus. i is bus and t is the time constraint is given below equation

$$0 \le Lsh_{i,t} \le L_{i,t} \quad (25)$$

2.5 AC Power flow constrains

The equation justifies the application of the law of conservation of energy at each bus for each interval.

$$\sum_{\Omega_i^{th}} P_{g,t} + Lhs_{i,t} + P_{i,t}^{w} + P_{i,t}^{s} + P_{i,t}^{dis} - P_{i,t}^{ch} - P_{i,t}^{L} = \sum_{\Omega_i^{l}} P_{ij,t} : \lambda_{i,t}^{p} \quad (26)$$

Locational marginal price ($\lambda_{i,t}$) at bus could also be calculated using equ. (26)

It is given by reactive power balance in Alternate Current -OPF and active and reactive power flow in the lines in equation (27-28).

$$\sum_{\Omega_i^{th}} Q_{g,t} - Q_{i,t}^{L} = \sum_{\Omega_i^{l}} Q_{ij,t} \quad (27)$$

$$P_{ij,t} = \frac{V_{i,t}^2}{z_{ij}}\cos\theta_{ij} - \frac{V_{i,t}V_{j,t}}{z_{ij}}\cos(\delta_{i,t} - \delta_{j,t} + \theta_{ij}) \quad (28)$$

$$Q_{ij,t} = \frac{V_{i,t}^2}{z_{ij}}\sin\theta_{ij} - \frac{V_{i,t}V_{j,t}}{z_{ij}}\sin\left(\delta_{i,t} - \delta_{j,t} + \theta_{ij}\right) - b\frac{V_{i,t}^2}{2} \quad (29)$$

Here impedance is given by $z_{ij} = \sqrt{{r_{ij}}^2 + {x_{ij}}^2}$

Active Power flow limit of the branches is described as:

$$-P_{ij}^{max} \le P_{ij,t} \le P_{ij}^{max} \quad (30)$$

The load angle and voltage angle at time for ith bus is constrained by:

$$-\pi/2 \le \delta_{i,t} \le \pi/2 \quad (31)$$

Reactive power flow limits are also considered in alternate Current -OPF:

$$-Q_{ij}^{max} \le Q_{ij,t} \le Q_{ij}^{max} \quad (32)$$

The voltage level at time for ith bus is constrained by:

$$0.95\text{p. u.} \le V_{i,t} \le 1.05\text{p. u.} \quad (33)$$

2.6 Conservation voltage reduction

For energy saving purpose, reducing the voltage magnitude intentionally at the distribution feeder to an allowable level is defined as conservation voltage reduction (CVR) also known as voltage optimization to manage demand during peak load hours and reduction in energy consumption through the year. Hence, voltage level at the end of line can be reduced within a permissible range (114–120 Volts) without damaging consumer appliances and other devices. CVR factor is defined in[33], to evaluate CVR effects. It measures the difference between the percentage change in voltage profiles and the percentage change in load consumption. expressed as:

$$CVR_f = \frac{\%\text{ Load change}}{\%\text{ Voltage change}} = \frac{(P_{base} - P_{cvr})/P_{base}}{(V_{base} - V_{cvr})/V_{base}} \quad (34)$$

P_{base} is base active load consumption and V_{base} is base voltage without CVR.

Time-varying voltage dependent load as proven by laboratory experiments, a strong voltage-dependence behavior is exhibited by the loads connected from low/medium voltage distribution network (VDN). Voltage magnitude and the load demand have a strong positive correlation. The voltage-sensitive load is to be modeled to study the potential CVR effect in the distribution network Dynamic load has been modeled in response. In previous such attempt Dynamic Motor Model and Composite Load Model is a combination of the static and dynamic motor load models were developed[34]. In this section, mathematical formulation of load models has been discussed and finally a time varying voltage dependent load has been modelled. Here PL and QL represents active and reactive power demand of the load, P_0 and Q_0 are their nominal value. V_{pu} is per unit voltage.Time varying ZIP Model[33]. The load is decomposed into its active and reactive parts as given by equation (35) and equation (36). Each part represented by three components, the constant impedance (Z), constant current (I), and the constant power (P) part.

$$P_{L,t} = P_0\left[\left(V_{pu,t}\right)^2/Z_p + V_{pu,t}I_p + P\right] \quad (35)$$

$$Q_{L,t} = Q_0\left[\left(V_{pu,t}\right)^2/Z_q + V_{pu,t}I_q + Q\right] \quad (36)$$

Where 1/Z+I+P ≈ 1.

PTI IEEE Model[35]: Active and reactive power part of the load is denoted by (37) and (38) which are both voltage and frequency dependent, according to this model.

$$P_{L,t} = P_0\left[a_1{V_{pu,t}}^{k1} + a_2{V_{pu.t}}^{k2} + a_3{V_{pu,t}}^{k3}\right](1 + a_4\Delta f) \quad (37)$$

$$Q_{L,t} = Q_0\left[a_5{V_{pu,t}}^{k4} + a_6{V_{pu,t}}^{k5} + a_7{V_{pu,t}}^{k6}\right](1 + a_8\Delta f) \quad (38)$$

Where Δf is the frequency deviation, which is the

difference between rated and actual frequencies. And $a_1+a_2+a_3 \approx 1$, $a_4+a_5+a_6 \approx 1$. According to comprehensive statistic studies, the load has been classified as: residential, commercial and industrial. And percentage values of residential (f_t^r), commercial (f_t^c) and industrial (f_t^i) load at each load node is time varying. Further, degree of voltage dependence of each of these categories is given by the exponents p^r, p^c, p^i, which are time invariant. Fractional load demand li,t specifies the fraction of maximum load desired at i^{th} bus at t^{th} time. Hence, time-varying voltage dependent load is modeled in order to precisely calculate the dynamic behaviors of load demand resulting from voltage changes at each time interval (e.g., 1 h in this paper) in equation (39) and equation (40).

Table 1.

gen	bus	Pmax k	Pmin kW	a(Rs/kW^2)	b(Rs/kW)	c(Rs)	Rup kW	RDp kW
g1	18	297	66	0.0102	0.547	5.82	47	47
g2	21	228	62	0.0102	0.547	5.82	45	45
g3	1	162	26.4	0.0216	1.332	13.66	24	24
g4	2	332	80.4	0.0216	1.332	13.66	54	54
g5	6	205	24.25	0.0258	1.497	15.67	35	35
g6	16	185	26.73	0.0203	1.052	10.81	31	31
g7	23	350	88.5	0.0203	1.052	10.81	55	55
g8	8	250	48	0.0204	1.089	11.32	45	45
g9	7	105	75	0.0297	1.726	8.01	49	49
g10	13	291	72.73	0.0306	1.693	8.27	46	46
g11	15	260	28.3	0.0301	1.711	7.77	45	45
g12	22	250	50	0.0186	0.988	10.19	43	43

$$P_{i,t}^{L} = l_{i,t} \times Pd_i^{max}\left[f_t^r(v_{i,t})^{pr} + f_t^c(v_{i,t})^{pc} + f_t^i(v_{i,t})^{pi}\right] \quad (39)$$

3. In addition, the following equality follows for AC power flow

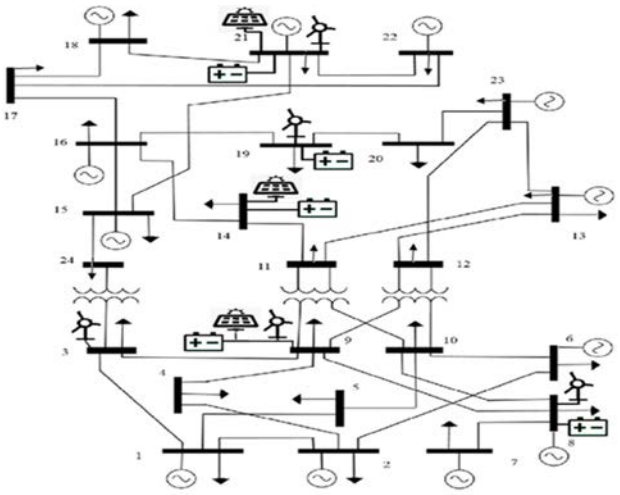

Fig. 2: Studied IEEE 24-bus test system

Table2. Network technical characteristics for 24 bus system.

Line	r(p.u.)	x(p.u.)	b(p.u.)	Limit (kW)
1.2	0.0261	0.0139	0.0461	175
1.3	0.3463	0.1212	0.0572	275
1.5	0.218	0.0845	0.0229	350
2.4	0.0328	0.0267	0.0343	275
2.6	0.397	0.1924	0.0526	200
3.9	0.0308	0.0197	0.0322	185
3.24	0.2315	0.0839	0.018	400
4.9	0.2686	0.1037	0.0281	225
5.1	0.2281	0.0883	0.0239	175
6.1	0.1395	0.0605	0.0459	250
7.8	0.1596	0.0614	0.0166	315
8.9	0.3273	0.1651	0.0447	200
8.1	0.3273	0.1651	0.0447	225
9.11	0.1235	0.0771	0.0211	350
9.12	0.1235	0.0771	0.0157	400
10.11	0.1577	0.0839	0.0263	300
10.12	0.1577	0.0839	0.0194	325
11.13	0.0613	0.0476	0.0999	310
11.14	0.0541	0.0418	0.0879	420
12.13	0.0619	0.0476	0.0999	500
12.23	0.1248	0.0966	0.0203	480
13.23	0.1113	0.0865	0.0181	460
14.16	0.0574	0.0389	0.0818	430
15.16	0.0226	0.0173	0.0364	511
15.21	0.0315	0.0245	0.0206	600
15.24	0.0674	0.0519	0.0109	400
16.17	0.0333	0.0259	0.0545	300
16.19	0.0325	0.0231	0.0485	250
17.18	0.0183	0.0144	0.0303	500
17.22	0.0135	0.0153	0.0221	400
18.21	0.0165	0.0129	0.0209	800
19.2	0.0255	0.0198	0.0166	750
20.23	0.0144	0.0108	0.0916	500
21.22	0.0875	0.0678	0.0242	400

Table3. Maximum capacity of the wind farms, solar farms and SOC^{max} of the batteries connected at various buses.

Bus	W_{cap}(kW)	S_{cap}(kW)	SOC^{max}(kWhr)
3	150	-	-
8	190	-	250
9	250	240	250
14	-	250	180
19	180	-	160
21	250	100	350

Table4. The maximum active and reactive load demand at each bus.

	Pd	Qd
1	108	22
2	97	20
3	150	37
4	74	15
5	71	14
6	136	28
7	125	25
8	271	35
9	155	36
10	165	30
11	126	28
12	122	25
13	265	54
14	194	39
15	317	64
16	100	20
17	75	15
18	333	68
19	281	37
20	128	26
21	211	23
22	249	51
23	132	29
24	75	15

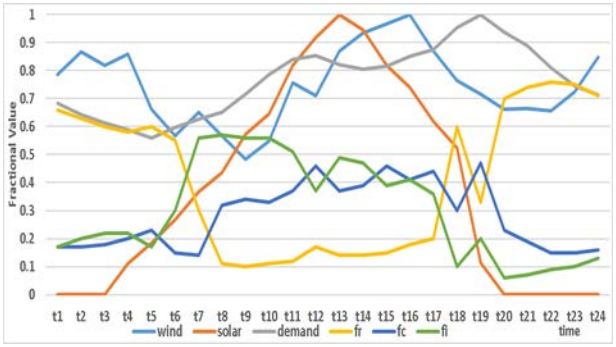

Fig. 3: Total fractional demand variation, wind and solar power availability with respect to time

Table 5 and Fig 3 show the daily variation of fractional demand for total, commercial and industrial load, fractional wind power availability and fractional solar power availability for each hour of the day. It is observed from the figure 3, the solar power is available from 3rd to 20th hours. The maximum solar power is available at 13th hour. The availability of the wind power is throughout the day, with a peak value at 16th hour and it is observed that the peak load is at 19th hour. Industrial and commercial loads are high, residential load is low during the office hours.

Table5. Variation of total fractional demand, wind and solar power availability w.r.t. time

Time	W	S	$l_{i,t}$	f_t^r	f_t^c	f_t^i
t1	0.786666	0	0.684511	0.66	0.17	0.17
t2	0.866666	0	0.644122	0.63	0.17	0.2
t3	0.817333	0	0.613069	0.6	0.18	0.22
t4	0.858666	0.11264	0.589733	0.58	0.2	0.22
t5	0.661333	0.18363	0.558874	0.6	0.23	0.17
t6	0.566666	0.26703	0.598018	0.55	0.15	0.3
t7	0.650666	0.36812	0.626786	0.3	0.14	0.56
t8	0.566666	0.43497	0.651743	0.11	0.32	0.57
t9	0.484891	0.57345	0.716039	0.1	0.34	0.56
t10	0.548229	0.64587	0.787007	0.11	0.33	0.56
t11	0.757333	0.81916	0.839016	0.12	0.37	0.51
t12	0.710666	0.91738	0.852733	0.17	0.46	0.37
t13	0.870666	1	0.820642	0.14	0.37	0.49
t14	0.934535	0.94371	0.804254	0.14	0.39	0.47
t15	0.966666	0.81946	0.816536	0.15	0.46	0.39
t16	1	0.73943	0.849394	0.18	0.41	0.41
t17	0.869333	0.61876	0.874071	0.2	0.44	0.36
t18	0.765333	0.52476	0.953615	0.6	0.3	0.1
t19	0.716666	0.11357	1	0.33	0.47	0.2
t20	0.661333	0	0.936368	0.7	0.23	0.06
t21	0.665333	0	0.887597	0.74	0.19	0.07

t22	0.656666	0	0.809297	0.76	0.15	0.09
t23	0.724457	0	0.745856	0.75	0.15	0.1
t24	0.848674	0	0.713473	0.71	0.16	0.13

4. Simulation Results and Discussions

Dell deskstop with Intel core i5-7500U CPU processor 2.4GHz The system is modeled as an NLP optimization problem with the microgrid operating independently under a significant voltage-dependent load. Optimization codes were used for the exeuation in GAMS build 24.4.3 software [49] by utilizing the CONOPT3 solver version 3.14W (Dec 13,2010 release).The problem is analysed for following different cases under full load conditions

Table.6 .Different case study ab

Case +Gen	**Description**
Case 1 (Gen)	Only diesel generators (DG) are considered.
Case2 (Gen+Bat)	DG s and Energy Storage Systems (ESS) together
Case3 (Gen+Res)	Renewable Energy Sources(RES) and DGs are considered.
Case4 (All In 1.0)	Energy Storage Systems(ESS) are considered along with RES and DGs. Here 1.0 indicates 100% load at each bus.

Case 4 is subdivided into further subcases depending upon the fractional change in load.

Case 4a (All In 0.9): Load is decreased by 10%.

Case 4b (All In 1.1): Load is increased by 10%.

Cost comparison of case 1-4 is given in Table 6 and is visualised by Fig 4. As expected, fuel cost and cost of loss of load is higher in case 1 and case 2 due to lack of power supply. Implementing BES increases cost of fuel but reduces the value of loss of load, which could be observed on comparing case 1 with case 2 and case 3 with case 4. It is also noted that voltage deviation increases slightly when the battery is applied along with the generators, when comparing case 1 and case 2 due to poor placement and underutilization of batteries. However it is quite opposite when comparing case 3 and 4. Voltage deviation in case 3 is highest among all other cases due to heavy injection of intermittent renewable power. BES system deals with this problem and hence in case 4 deviation is lowest among all because batteries are placed at optimal locations. Congestion cost is higher in case 3 and 4 in comparison to case 1 and 2 which is justified by the fact that more power is available for distribution when RES are utilised, and hence the lines will be heavily loaded. Similarly, with use of BES congestion cost increases as observed comparing case 1 with case 2 and it decreases as observed on comparing case 3 with case 4.

Table.7. Cost comparision of different cases of energy availability (Case 1-4)

	GEN	**GEN+BAT**	**GEN+RES**	**ALL IN 1.0**
Fcost	348962.008	354648.910	224580.675	226668.382
VoLL	260463.230	250551.876	65742.351	53772.710
Vdev	35090.026	35355.144	36623.767	35000.007
Congestion cost	76528.006	77094.074	121943.014	100669.042
Total Cost	644518.047	640556.064	326946.088	315441.018
LMP	15.12468667	15.07770333	10.14040625	10.38940972

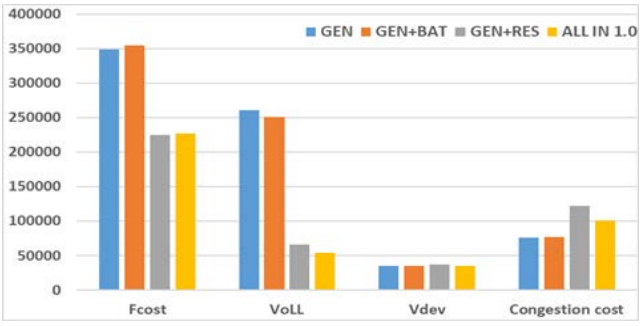

Fig. 4: Cost comparision of different cases of energy

Similarly, cost comparison of case 4, 4a, 4b is given in Table 7 and is visualised by Fig 5. As expected when the load increases, fuel cost, and load shedding and voltage deviation also increases. But the congestion cost decreases because smaller amount of power is available to dispatch, and hence lines are lightly loaded.

Table.8.*Cost comparisons of different fraction of load at each bus in* case ALL IN (Case 4,4a,4b*)*

	All In 0.9	**All In 1.0**	**All In 1.1**
Fcost	177198.929	226668.382	278265.253
V_{oLL}	34368.844	53772.710	83406.975
V_{dev}	34049.399	35000.007	36406.492
Congestion cost	109940.057	100669.042	92322.056
Totol Cost	245549.095	315441.018	398078.073
LMP	8.8013125	10.38940972	12.09801167

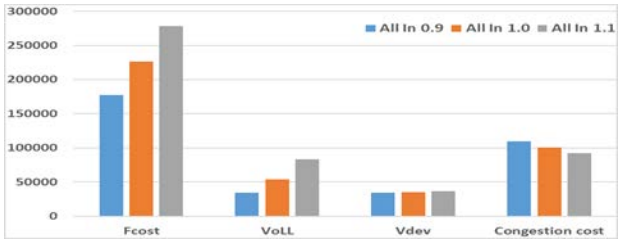

Fig. 5: Cost comparisons of different fraction of load at each bus in case ALL IN (Case 4,4a,4b)

Since penalty for the loss of renewable energy is quite high in the objective function, RES are fully utilized when it is available. There is no wind power or solar power curtailment throughout the operation of the Microgrid. Hence the cost of loss of renewables is also zero in each case. And so, it is not included in the table

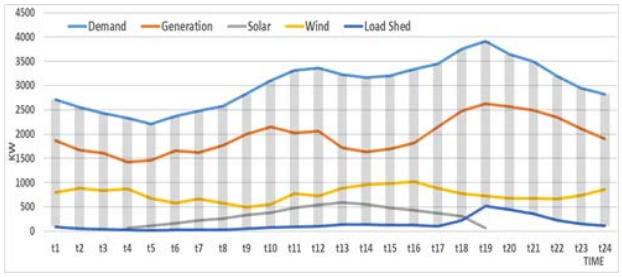

Fig. 6: Dispatch schedule for case 3 (Gen+Res)

Figures below show the dispatch schedule for different cases of energy availability.

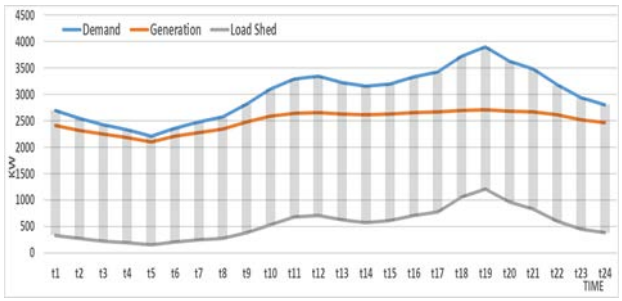

Fig. 7: Dispatch schedule for case 1 (Gen)

For case 1, Fig 6 shows that load shedding is inevitable since LMP at various buses exceeds VOLL. Generator are operating at maximum limits between t11 and t20. Both load and load shedding occurs at t19

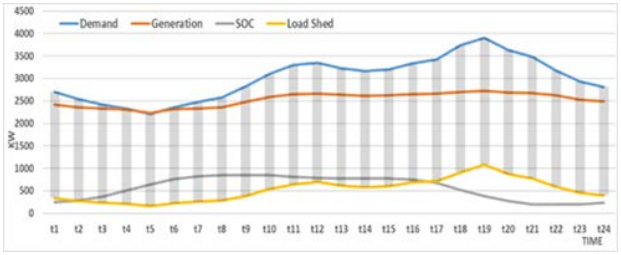

Fig. 8: Dispatch schedule for case 2 (Gen+Bat)

For case 2 shown by Fig 7, generator were operating at maximum limits for most of the time, since generated energy is stored in battery. It was observed that batteries at bus 9 and bus 14 remains unutilized due to lack of energy availability. Load shedding dropped by little amount and is still maximum at t19

For case 3 shown by Fig 8, diesel generation as well as load shedding has dropped to a great extent, when solar and wind power are available. Renewable energy is fully utilized. Load shedding is still maximum at t19 when the solar power drops to almost zero.

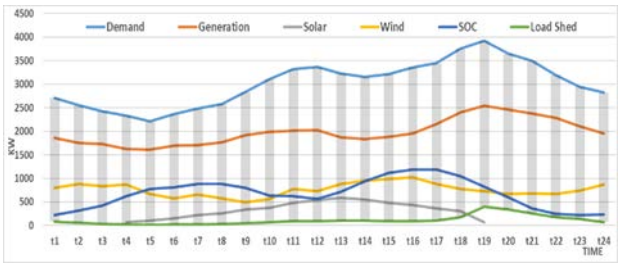

Fig. 9: Dispatch schedule for case 4 (All In 1.0)

In case 4 shown by Fig 9, the curve of generation smoothens with integration of BES. Battery acts as a load when SOC increases and as a source when SOC decreases. Renewable energy is fully utilized. Again, load shedding is still maximum at t19.

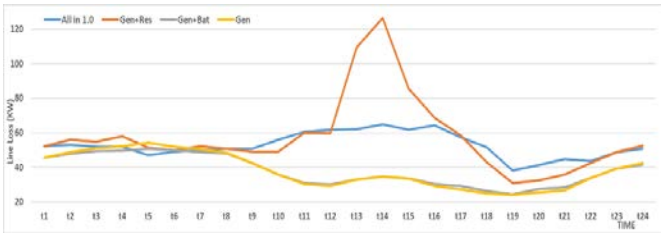

Fig. 10: Line losses (totaled over buses) for different cases of energy availability (Case 1-4)

The Fig 10 explains the following few points. With the availability of renewable energy, the power transferred through the lines increases in case 3 and 4, and hence line losses are more. In addition, the EES plays an important role in reducing the line losses which could be observed on comparing Case 3 and Case 4. Comparing Case 1 and Case 2 gives a clear idea that ESS remains unused when there is lack of energy sources.

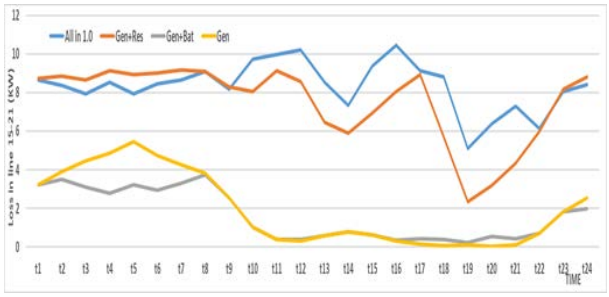

Fig. 11: Active power loss in line 9-12 for different cases of energy availability (Case 1-4)

Fig 11 shows that power transferred from bus 9 to bus 12 and from bus 21 to bus 15 is high in case 3 and case 4 due to availability of renewables. Fig 12 and Fig 13 show that power transferred from bus 23 to bus 20 is high in case 1 and case 2 due to lack of renewable energy and large generation capability available at bus 23

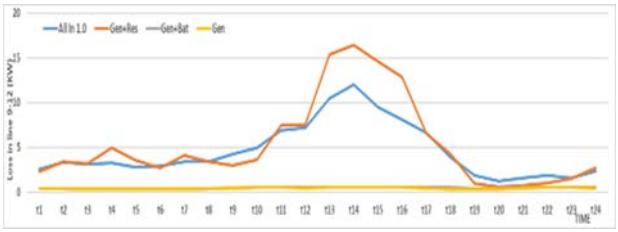

Fig. 12: Active power loss in line 15-21 for different cases of energy availability (Case 1-4)

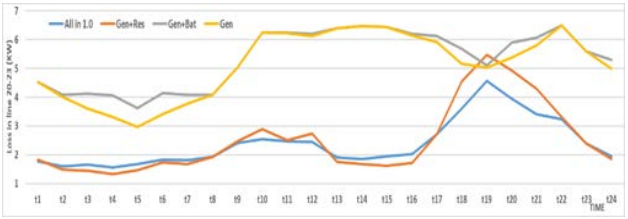

Fig. 13: Active power loss in line 20-23 for different cases of energy availability (Case 1-4)

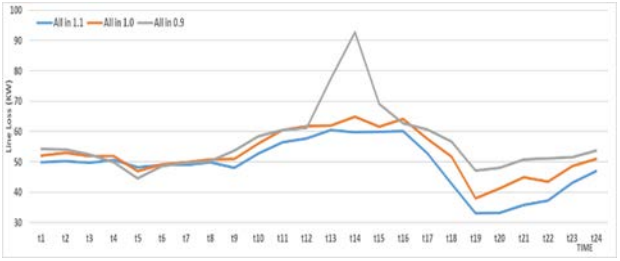

Fig. 14: Line losses (totaled over buses) for different fraction of load at each bus in case ALL IN (Case 4,4a,4b)

In Fig 14, it could be observed that when load was decreased by 10% the line losses increases at 13-15th hour due to availability of excess wind and solar power. Similarly, when load was increased by 10%, line losses decreases because of lack of dispatchable power.Voltage at each bus is calculated by power flow equations (28),(29) and is limited by constrain (33). Variation in voltage is strictly limited because of including voltage deviation cost in the objective function (5) and because of shedding of the non-critical loads (25). Since the load is voltage dependent, it was expected that voltage at different buses should be close to 0.95 p.u. (i.e. maintaining a high CVR_f) in order to minimize load and hence the cost of the objective function. But we have also considered cost of voltage deviation in the cost function and hence the voltages are close to 1 p.u. and hence the CVR_f is low.

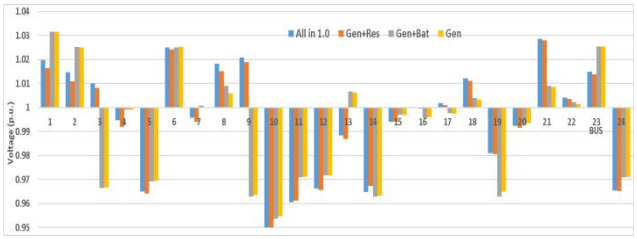

Fig. **15:** Voltage p.u. at each bus (averaged over time) for different cases of energy availability (Case 1-4)

The Fig 15 clearly shows that voltage variation for case 1 and 2 are similar due to unavailability of RES and that in case 3 and 4 are similar due to its availability. There is no specific trend followed by voltage variation. But the pattern could be observed if we study Fig 11-13 and Fig 15 together. As RES is available, significant power is transferred from bus 9 to bus 12 and from bus 21 to bus 15 and hence voltage at bus 9 and 21 is high and that at bus 12 and 15 is slightly low when comparing case 3 or 4 with case 1 or 2. Similarly, when RES is unavailable, high generated power transferred from bus 23 to bus 20 and hence voltage at bus 23 is higher in case 1 and 2 as compared to case 3 and 4.

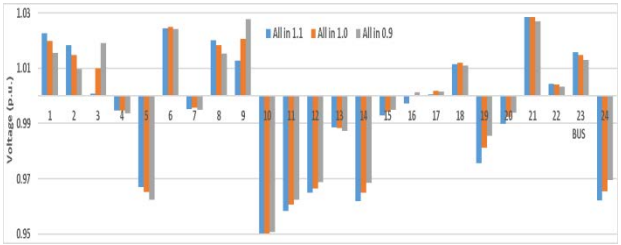

Fig.16: Voltage p.u. at each bus (averaged over time) for different fraction of load at each bus with ALL IN (Case 4,4a,4b)

Fig 16 shows that the voltage deviation generally decreases with decrease in load. It is also observed from the Fig 15 and Fig 16 that bus number 10 has the lowest p.u. voltage. This is due to the fact that there is little reactive power support at bus 10, hence it should have low voltage to receive active and reactive power from other buses. Since, a voltage dependent load has been modelled, low p.u. voltage will reduce active and reactive power

demand at any bus.

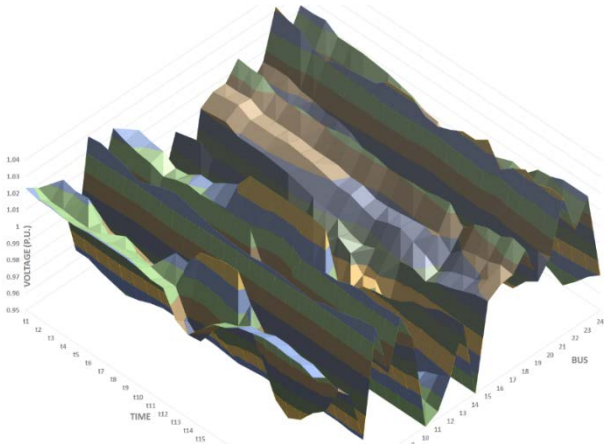

Fig. 17: Voltage profile for case 4 (ALL IN case with fractional load 1.0

A surface plot showing variation of voltage at different bus with respect to time for case 4 is shown in the Fig 17.

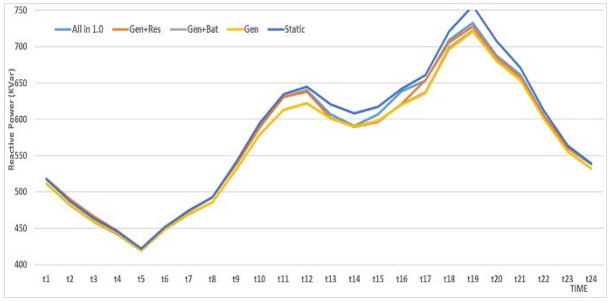

Fig.18: Variation in reactive power demand due to time varying voltage for different cases of energy availability (Case 1-4)

From Fig 18 it is observed that the variation in reactive power demand is limited by limiting variation in voltage (i.e. maintaining a low CVR_f). It could be seen that reactive power demand would have been slightly higher if the load was static. Since exponents of reactive power in

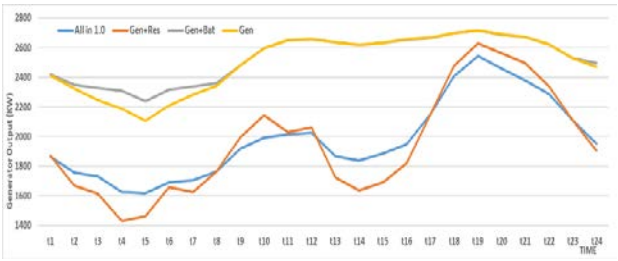

Fig. 19: Comparison of generator output for different cases of energy availability (Case 1-4)

voltage dependent load model are greater than that of active power, variation in active power is negligible.

Fig 19 shows the generation schedule for various cases. Generators are operating at the maximum limits in case 1 and case 2. However, generation drops to a considerable extent when RES is employed in case 3 and case 4

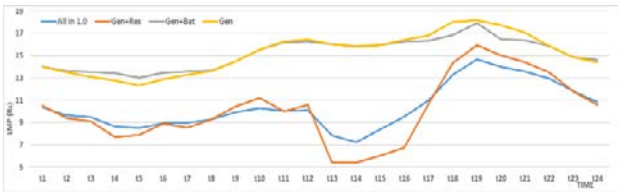

Fig. 20: Comparison of generator output for different cases of energy availability (Case 1-4)

Fig 19 and Fig 20 shows that LMP is high for case 1 and case 2. Also, LMP is low for case 3 and case 4 due to availability of RES. Further ESS smoothens the LMP curve, variation in LMP is minimized

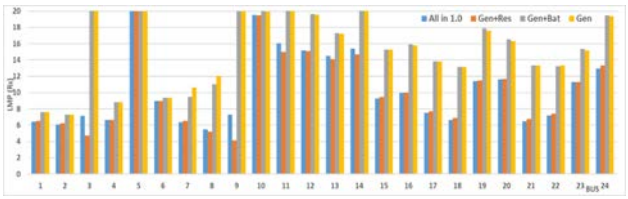

Fig. 21: LMP (averaged over time) at each bus for different cases of energy availability (Case 1-4)

The Fig 21 shows that LMP at bus 5 and bus 10 remains high in all the cases due to lack of availability of energy sources and hence load shedding at these buses is inevitable because VOLL is Rs 20. Hence whenever LMP equals or exceeds VOLL, load shedding occurs. Whenever the RES are operational, LMP at most of the buses falls significantly

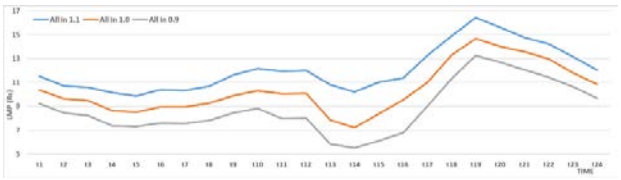

Fig. 22: LMP (averaged over buses) wrt. time for different fraction of load at each bus with ALL IN (Case 4,4a,4b)

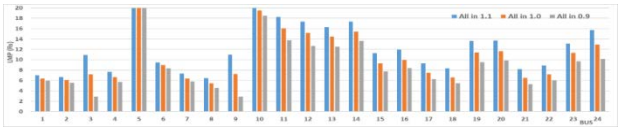

Fig. 23: LMP (averaged over buses) wrt. time for different fraction of load at each bus with ALL IN (Case 4,4a,4b)

As expected, Fig 22 and Fig 23 show that LMP is high when fractional load is 1.1 and low when fractional load is 0.9.

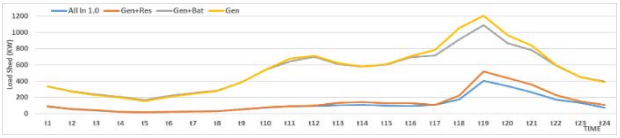

Fig. 24: Load shedding wrt. time in different cases of energy availability (Case 1-4)

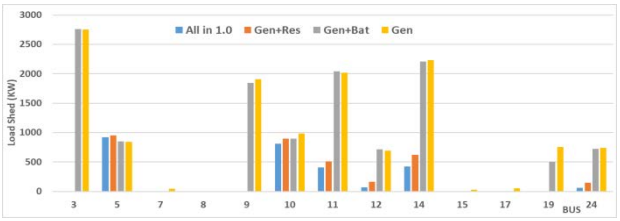

Fig. 25: Load shedding (totaled over time) at each bus for different cases of energy availability (Case 1-4)

Fig 24 and Fig 25 shows that load shedding drops significantly on employing RES and it drops slightly when ESS is employed. Further Fig 25 shows that there is no significant change in LMP or Load shedding at bus 5 and bus 10, because of lack of availability of power.

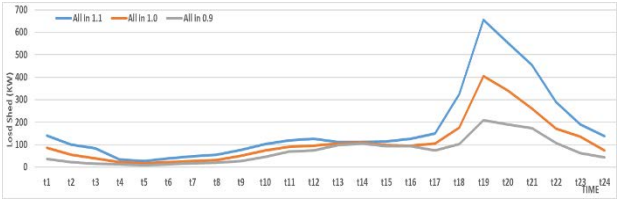

Fig. 26: Load shedding for different fraction of load at each bus in case ALL IN (Case 4,4a,4b)

As expected, Fig 26 shows load shedding is high when fractional load is 1.1 and low when it is 0.9.

As seen in the dispatch schedule, both Fig 25 and Fig 26 shows the variation of load shedding w.r.t. time which is maximum in 19th hour of peak load for all the cases. Also, there is huge drop in the available solar power in the 19th hour.

5. Conclusions

The proposed technique have shown the optimal utilization of all the resources available in the MG and meticulously considered the aspects such as voltage profile improvement and power loss reduction. Different cases and scenarios are tested through the proposed algorithm and the output has emphasized the correctness, effectiveness and robustness of the model. It is observed and can be concluded that heavy load shedding occurs when no support is provided by RES and hence voltage profile is maintained even when there is lack of power supply.Proposed economic dispatch model (ED) integrates RES to the MG, taking into account the intermittency and uncertainty of wind and solar energy resources. The developed methodology have reflects the maximum conversion of renewable power into active power and hence reduce conventional power generation and fuel cost. It is observed that voltage deviation increases at buses where RES is deployed. Further, BES aids the situation by solving the problem of intermittency of RES. Hence role of BES in fuel cost reduction and in improving flexibility of the MG by dealing with intermittent nature RES is explained. Parameters like LMP and congestion cost are proved to be useful in monitoring and maintaining the system performance even in the worst possible contingency. LMP is an important parameter which could solve optimal siting and sizing problem effectively avoiding usage of computation intensive algorithms. Further, it is seen that congestion cost increases with increase in power supply or decrease in load because in both these cases more power will be available for distribution through the lines. Instead of a static load model, a time varying voltage dependent load has been simulated and hence CVR is achieved. It was expected that voltage level at most of the buses will drop down to minimum possible value ie 1.05 pu. But cost function defined for minimizing voltage deviation is included in the objective function and hence voltage levels are brought back to 1 pu.

Reference

1) R.A. Jessam, “Experimental study of wind turbine power generation utilizing discharged air of air conditioner blower,” *Evergreen*, **9** (*4*) 1103–1109 (2022). doi:10.5109/6625722.
2) T.E. Hoff, H.J. Wenger, and B.K. Farmer, “Distributed generation: an alternative to electric utility investments in system capacity,” *Energy Policy*, **24** (*2 SPEC. ISS.*) 137–147 (1996). doi:10.1016/0301-4215(95)00152-2.
3) M.M. Rahman, S. Saha, M.Z.H. Majumder, T.T. Suki, M.H. Rahman, F. Akter, M.A.S. Haque, and M.K. Hossain, “Energy conservation of smart grid system using voltage reduction technique and its challenges,” *Evergreen*, **9** (*4*) 924–938 (2022). doi:10.5109/6622879.
4) H.A. Jaffar, A.A. Ismaeel, and A.L. Shuraiji, “Review of hybrid photovoltaic- air updraft solar application: present and proposed state models,” *Evergreen*, **9** (*4*) 1181–1202 (2022). doi:10.5109/6625729.
5) A. Dhiman, and G. Sachdeva, “Energy and exergy analysis of a pressurized solar cooking system based on a parabolic dish collector,” *Evergreen*, **9** (*4*) 1168–1180 (2022). doi:10.5109/6625728.
6) R.G. Wandhare, and V. Agarwal, “Novel integration of a pv-wind energy system with enhanced efficiency,” *IEEE Trans. Power Electron.*, **30** (*7*) 3638–3649 (2015). doi:10.1109/TPEL.2014.2345766.
7) M. Ayundyahrini, D.A. Susanto, H. Febriansyah, F.M. Rizanulhaq, and G.H. Aditya, “Smart farming: integrated solar water pumping irrigation system in thailand,” *Evergreen*, **10** (*1*) 553–563 (2023). doi:10.5109/6782161.
8) R. Kumar, and A. Agarwal, “Space vector modulation for

nine-switch converter employing three phase loads," **10** (*02*) 1034–1040 (2023).

9) J. Liu, W. Fang, X. Zhang, and C. Yang, "An improved photovoltaic power forecasting model with the assistance of aerosol index data," *IEEE Trans. Sustain. Energy*, **6** (*2*) 434–442 (2015). doi:10.1109/TSTE.2014.2381224.
10) M.J.E. Alam, K.M. Muttaqi, and D. Sutanto, "Mitigation of rooftop solar pv impacts and evening peak support by managing available capacity of distributed energy storage systems," *IEEE Trans. Power Syst.*, **28** (*4*) 3874–3884 (2013). doi:10.1109/TPWRS.2013.2259269.
11) R. Kumar, R. Sharma, and A. Kumar, "Adaptive negative impedance strategy for stability improvement in dc microgrid with constant power loads," *Comput. Electr. Eng.*, **94** (*July*) 107296 (2021). doi:10.1016/j.compeleceng.2021.107296.
12) S. Ghosh, S. Rahman, and M. Pipattanasomporn, "Power curtailment with pv inverters and solar," *IEEE Trans. Sustain. Energy*, **8** (*1*) 13–22 (2017).
13) P. Chiradeja, "Benefit of distributed generation: a line loss reduction analysis," *Proc. IEEE Power Eng. Soc. Transm. Distrib. Conf.*, **2005** 1–5 (2005). doi:10.1109/TDC.2005.1546964.
14) V. Trivedi, A. Saxena, M. Javed, P. Kumar, and V. Singh, "Design of six seater electrical vehicle (golf cart)," **10** (*02*) 953–961 (2023).
15) T.C. Rudien, D.H. Didane, M.F.M. Batcha, K. Abdullah, S. Mohd, B. Manshoor, and S. Al-Alimi, "Technical feasibility analysis of wind energy potentials in two sites of east malaysia: santubong and kudat," *Evergreen*, **8** (*2*) 271–279 (2021). doi:10.5109/4480703.
16) H. Zhang, D. Yue, and X. Xie, "Robust optimization for dynamic economic dispatch under wind power uncertainty with different levels of uncertainty budget," *IEEE Access*, **4** 7633–7644 (2016). doi:10.1109/ACCESS.2016.2621338.
17) B. Bahmani-Firouzi, E. Farjah, and R. Azizipanah-Abarghooee, "An efficient scenario-based and fuzzy self-adaptive learning particle swarm optimization approach for dynamic economic emission dispatch considering load and wind power uncertainties," *Energy*, **50** (*1*) 232–244 (2013). doi:10.1016/j.energy.2012.11.017.
18) C. Peng, H. Sun, J. Guo, and G. Liu, "Dynamic economic dispatch for wind-thermal power system using a novel bi-population chaotic differential evolution algorithm," *Int. J. Electr. Power Energy Syst.*, **42** (*1*) 119–126 (2012). doi:10.1016/j.ijepes.2012.03.012.
19) B.R. Pereira, G.R.M. Martins Da Costa, J. Contreras, and J.R.S. Mantovani, "Optimal distributed generation and reactive power allocation in electrical distribution systems," *IEEE Trans. Sustain. Energy*, **7** (*3*) 975–984 (2016). doi:10.1109/TSTE.2015.2512819.
20) H.E. Farag, and S.M. Kandil, "Optimum planning of renewable energy resources in conjunction with battery energy storage systems," *2015 4th Int. Conf. Electr. Power Energy Convers. Syst. EPECS 2015*, (2015). doi:10.1109/EPECS.2015.7368491.
21) M.S. Srinivas, "Distribution load flows: a brief review," *2000 IEEE Power Eng. Soc. Conf. Proc.*, **2** (*c*) 942–945 (2000). doi:10.1109/PESW.2000.850058.
22) P.M. De Oliveira-De Jesús, and M.T. Ponce De Leão, "Distribution loss allocation methods assessment under electricity market environment," *2005 IEEE Russ. Power Tech, PowerTech*, 1–7 (2005). doi:10.1109/PTC.2005.4524630.
23) S.S. AlKaabi, V. Khadkikar, and H.H. Zeineldin, "Incorporating pv inverter control schemes for planning active distribution networks," *IEEE Trans. Sustain. Energy*, **6** (*4*) 1224–1233 (2015). doi:10.1109/TSTE.2015.2422305.
24) V. Kekatos, G. Wang, A.J. Conejo, and G.B. Giannakis, "Stochastic reactive power management in microgrids with renewables," *IEEE Trans. Power Syst.*, **30** (*6*) 3386–3395 (2015). doi:10.1109/TPWRS.2014.2369452.
25) B.W. Kennedy, and R.H. Fletcher, "Conservation voltage reduction (cvr) at snohomish county pud," *IEEE Trans. Power Syst.*, **6** (*3*) 986–998 (1991). doi:10.1109/59.119238.
26) Z. Wang, B. Chen, J. Wang, and M.M. Begovic, "Stochastic dg placement for conservation voltage reduction based on multiple replications procedure," *IEEE Trans. Power Deliv.*, **30** (*3*) 1039–1047 (2015). doi:10.1109/TPWRD.2014.2331275.
27) Y. Zhang, S. Ren, Z.Y. Dong, Y. Xu, K. Meng, and Y. Zheng, "Optimal placement of battery energy storage in distribution networks considering conservation voltage reduction and stochastic load composition," *IET Gener. Transm. Distrib.*, **11** (*15*) 3862–3870 (2017). doi:10.1049/IET-GTD.2017.0508.
28) M. Manbachi, B. Shahabi, H. Farhangi, and A. Palizban, "Real-time adaptive vvo / cvr topology using," *IEEE Trans. Sustain. Energy*, **5** (*2*) 587–597 (2014).
29) C.Z. El-Bayeh, K. Alzaareer, B. Brahmi, and M. Zellagui, "A novel algorithm for controlling active and reactive power flows of electric vehicles in buildings and its impact on the distribution network," *World Electr. Veh. J.*, **11** (*2*) 1–20 (2020). doi:10.3390/WEVJ11020043.
30) M. Nemati, M. Braun, and S. Tenbohlen, "Optimization of unit commitment and economic dispatch in microgrids based on genetic algorithm and mixed integer linear programming," *Appl. Energy*, **210** 944–963 (2018). doi:10.1016/j.apenergy.2017.07.007.
31) R. Chedid, H. Akiki, and S. Rahman, "A decision support technique for the design of hybrid solar-wind power systems," *IEEE Trans. Energy Convers.*, **13** (*1*) 76–83 (1998). doi:10.1109/60.658207.
32) F. Nazari-Heris, B. Mohammadi-ivatloo, and D. Nazarpour, "Network constrained economic dispatch of renewable energy and chp based microgrids," *Int. J. Electr. Power Energy Syst.*, **110** (*March*) 144–160 (2019). doi:10.1016/j.ijepes.2019.02.037.
33) Y. Zhang, Y. Xu, H. Yang, and Z.Y. Dong, "Voltage regulation-oriented co-planning of distributed generation and battery storage in active distribution networks," *Int. J. Electr. Power Energy Syst.*, **105** (*August 2018*) 79–88 (2019). doi:10.1016/j.ijepes.2018.07.036.
34) W.S. Kao, C.T. Huang, and C.Y. Chiou, "Dynamcl load

modeling in taipower system stability studies," *IEEE Trans. Power Syst.*, **10** (*2*) 907–914 (1995). doi:10.1109/59.387933.

35) J.C. Wang, H.D. Chiang, C.L. Chang, A.H. Liu, C.H. Huang, and C.Y. Huang, "Development of a frequency-dependent composite load model using the measurement approach," *IEEE Trans. Power Syst.*, **9** (*3*) 1546–1556 (1994). doi:10.1109/59.336105.